

THE NONLINEAR DYNAMIC RESPONSE ANALYSIS OF FRAME-SUPPORTED MULTI-RIBBED SLAB STRUCTURE

TIAN Jie¹, YAO Qianfeng² and Huang Wei³

¹ Associate Professor, Dept. of Civil Engineering, Xi'an University of Technology, Xi'an, China

² Professor, School of Civil Engineering, Xi'an University of Architecture & Technology, Xi'an, China

³ Associate Professor, School of Civil Engineering, Xi'an University of Architecture & Technology, Xi'an, China

Email: tianjie@xaut.edu.cn, yaoqf808@163.com, qqhuangwei2005@126.com

ABSTRACT:

In this paper nonlinear dynamic analysis model of frame-supported multi-ribbed slab structure (FSMRSS) is established with a rigid frame-oblique compression bar macro-model, which bottom frame and upper inner frame of multi-ribbed wall slab as well as outer frame are simulated by beam and column elements with retrogressive three-linear resilience model, while an analytical macro-model based on an equivalent strut approach integrated with a smooth hysteretic model is proposed for representing silicate brick infill panels. The hysteresis model uses degrading control parameters for stiffness and strength degradation and slip pinching. The nonlinear dynamic time-history analysis of 14 numerical cases of FSMRSS under eight earthquakes has been carried out. The dynamic response as well as influencing factors of FSMRSS was carefully studied, which provides more data information for the comprehension of earthquake responses characteristic of the structures. FSMRSS shows generally good seismic performance to severe earthquake motions.

KEYWORDS: Frame-supported multi-ribbed slab structure (FSMRSS), rigid frame-oblique compression bar macro-model, nonlinear dynamic time-history analysis

1. INTRODUCTION

Frame-supported multi-ribbed slab structure (FSMRSS) is composed of bottom frame and upper multi-ribbed slab structure, while upper multi-ribbed slab structure is composed of multi-ribbed wall slab being buildup of reinforced concrete inner frame (made up of rib beams and rib columns) with infilled silicate bricks and outer frame. Because load-bearing mechanism and constitution connecting of FSMRSS is complex, specially there is a matching problem of bearing capacity and stiffness in the transform storey of FSMRSS, it is highly important for study of seismic performance of the FSMRSS. In this paper, the nonlinear dynamic calculating model of the FSMRSS was established. The dynamic response of the structure under horizontal earthquakes was carefully studied, which provides more data information for the comprehension of earthquake responses behavior of the structures.

2. THE NONLINEAR DYNAMIC ANALYSIS METHOD OF FSMRSS

2.1 Structural Analysis Model

The bottom frame of frame-supported multi-ribbed slab structure (FSMRSS) can be modeled by a system of pole most commonly used in frame structure. The upper multi-ribbed slab structure has an analogy with a miniature infill frame. Drawing an analogy between them, there is a similarity of the failure mode and deformation features and mechanics characteristic. For simplicity, and combining the results of experimental study and FEM analysis of multi-ribbed wall slab as well as FSMRSS, the proposed analytical development assumes that the contribution of the silicate brick infill panel to the response of the infilled frame can be replaced by a system of two diagonal silicate brick compression struts. Considering a fundamental infilled frame element with infilled silicate brick shown in Figure 1, based on the model of masonry infill panel (Madan and Reinhorn et al., 1997), an equivalent strut model for silicate brick infill panels in multi-ribbed wall slab was

presented. Since the tension strength of silicate brick is negligible, the individual silicate brick strut is considered to be ineffective in tension. However, the combination of both diagonal struts provides a lateral load resisting mechanism for the opposite lateral directions of loading.

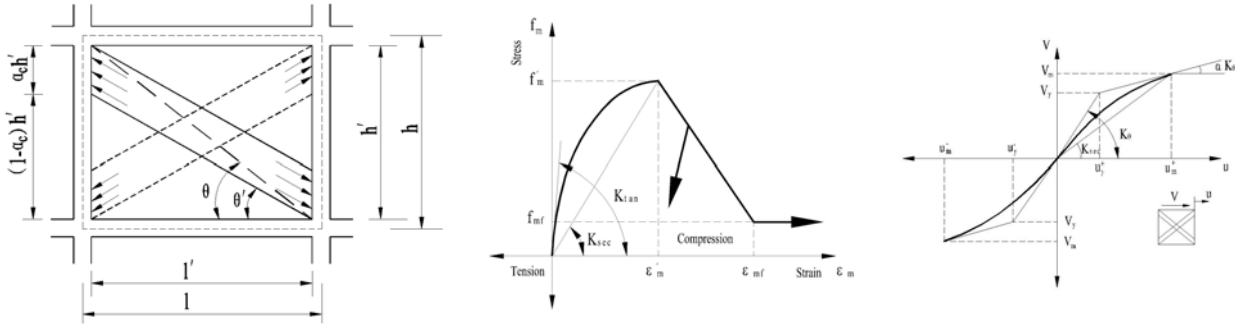


Figure 1 Equivalent strut model Figure 2 Constitutive model for silicate brick Figure 3 Strength envelope for silicate brick infill panel

The stress-strain relationship for silicate brick in compression is commonly idealized using a parabolic function (Reinhorn et al., 1995) until the peak stress f'_m is reached, then it is assumed to drop linearly with increasing strain to a small fraction of the peak value, and then remains constant at this value of stress (see Figure 2). The lateral force-deformation relationship for the silicate brick infill panel is assumed to be a smooth curve boundary by a bilinear strength envelope with an initial elastic stiffness until the yield force V_y and there on a post-yield degraded stiffness until the maximum force V_m is reached (see Figure 3). The corresponding lateral displacement values are denoted as u_y and u_m respectively, the maximum lateral force V_m and the corresponding displacement u_m are calculated as (Saneinejad and Hobbs, 1995):

$$V_m^+(V_m^-) \leq A_d f'_m \cos \theta \leq \frac{\nu l'}{(1 - 0.45 \tan \theta') \cos \theta} \leq \frac{0.83 t l'}{\cos \theta} \quad (2.1)$$

$$u_m^+(u_m^-) = \frac{\epsilon'_m L_d}{\cos \theta} \quad (2.2)$$

in which t = thickness of the infill panel; l' = lateral dimension of the infill panel; f'_m = silicate brick prism strength; ϵ'_m = corresponding strain; θ = inclination of the diagonal strut; ν = basic shear strength of silicate brick; and A_d and L_d = area and length of the equivalent diagonal strut respectively, calculated as (Saneinejad and Hobbs, 1995):

$$A_d = (1 - \alpha_c) \alpha_c t h' \frac{\sigma_c}{f_c} + \alpha_b t l' \frac{\tau_b}{f_c} \leq \frac{0.5 t h' f_a / f_c}{\cos \theta} \quad (2.3)$$

$$L_d = \sqrt{(1 - \alpha_c)^2 h'^2 + l'^2} \quad (2.4)$$

where the quantities α_c , α_b , σ_c , τ_b , f_a and f_c , depending on the geometric and material properties of the frame and infill panel, can be estimated using the formulations of the equivalent strut model proposed by Saneinejad et al. (1995).

The monotonic lateral force-displacement curve is completely defined by the maximum force V_m , corresponding displacement u_m , initial stiffness K_0 , and the ratio α of the post-yield to initial stiffness. The initial stiffness K_0 of the infill silicate brick panel may be estimated using the following proposed formula:

$$K_0 = 2 \frac{V_m}{u_m} \quad (2.5)$$

The lateral yield force and displacement of the infill panel can be calculated from (Reinhorn et al., 1995):

$$V_y^+(V_y^-) = \frac{V_m - \alpha K_0 u_m}{1 - \alpha} \quad (2.6)$$

$$u_y^+ (u_y^-) = \frac{V_m - \alpha K_0 u_m}{K_0 (1 - \alpha)} \quad (2.7)$$

2.2 Dynamic Analysis Equation

The nonlinear dynamic analysis was done using IDARC2D Version 6.1(Reinhorn et al., 2006), and was carried out using a combination of the Newmark-Beta integration method and the pseudo-force method. The solution was carried out in incremental form, according to:

$$[M]\{\Delta\ddot{u}\} + [C]\{\Delta\dot{u}\} + [K_t]\{\Delta u\} = -[M]\{I\}\Delta\ddot{x}_g - \{\Delta P_{IW}\} + c_{corr}\{\Delta F_{err}\} \quad (2.8)$$

where $[M]$ is the lumped mass matrix of the structure; $[C]$ is the viscous matrix of the structure; $[K_t]$ is the tangent stiffness matrix; $\{\Delta u\}$, $\{\Delta\dot{u}\}$, and $\{\Delta\ddot{u}\}$ are the incremental vectors of displacement, velocity and acceleration in the structure, respectively; $\{I\}$ is the unit vector; $\Delta\ddot{x}_g$ is the increment in the horizontal ground acceleration; $\{\Delta P_{IW}\}$ is the restoring force from infill panels; c_{corr} is a correction coefficient (usually taken as one); $\{\Delta F_{err}\}$ is the vector with the unbalanced forces in the structure.

The bottom frame and upper inner frame of multi-ribbed wall slab as well as outer frame were simulated by beam and column elements integrated with retrogressive three-linear resilience model, while silicate brick infill panels were simulated by infill panel elements integrated with a smooth hysteretic model, the hysteretic model used degrading control parameters for stiffness and strength degradation and slip pinching.

2.3 Choosing of Input Earthquake Ground Motions

The 8 natural earthquake ground motions were chosen from the China Strong Motion Database and PEER Strong Motion Database mainly considering magnitude, site condition, PGA, PGV and PGA/PGV. The selected records are shown in Table 2.1. The response spectrums of the selected records are shown in Figure 4.

Table 2.1 Input earthquake ground motions

Earthquake	File name	Station	Comp.	Mag. (Ms)	PGA (g)	PGV (cm/s)	PGA /PGV	Duration	
1	Imperial Valley(1940)	ELC	El Centro Array #9	S00E	6.7	0.342	33.5	1.02	53.76
2	Kern County(1952)	TAFT	Taft Lincoln School	S69E	7.7	0.176	17.7	0.99	54.40
3	Northridge(1994)	NORE	Arleta-Nordhoff Fire Sta	ARL090	6.7	0.344	40.6	0.85	40.00
4	San Fernando(1971)	SFERT	Castaic-Old Bridge Route	ORR021	6.6	0.324	15.6	2.08	61.80
5	Loma Prieta (1989)	LPRI	SF - Presidio	PRS090	7.1	0.201	32.4	0.62	39.95
6	Coalinga(1983)	COAA	Parkfield -Fault Zone 14	H-Z14090	6.5	0.274	28.3	0.97	40.00
7	Kobe(1995)	KOBE	Shin-Osaka	SHI000	7.2	0.243	37.8	0.64	40.96
8	Friuli, Italy(1976)	FRIT	Tolmezzo	A-TMZ270	6.5	0.315	30.8	1.02	36.35

3. THE NONLINEAR EARTHQUAKE RESPONSES ANALYSIS OF FSMRSS

3.1 Calculating Model

Calculating models chose 14 plane frame-supported multi-ribbed slab structures with single span or double spans frame-supported storey. The typical elevation of calculating model structures is shown in Figure 5. The thickness of multi-ribbed slab is 200mm, width and highness dimension of rib beams and rib columns are

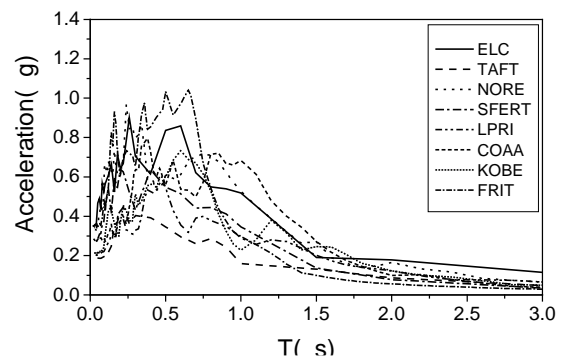


Figure 4 Response spectrums of the selected records (damping ratio of 5%)

200×100mm, hidden beams are 200×300 mm, top beams are 200×500mm, outer frame columns are 200×400mm. Concrete strength grade of rib beams and rib columns is C20, hidden beams and top beams and outer frame columns are C25, bottom frame is C30. Analysis parameter is height to span ratio of trimmer beam h/l , width to span ratio of frame-supported columns b/l , width to highness ratio of frame-supported columns b/H , height to span ratio of second storey multi-ribbed wall slab h_w/l and landscape orientation shear stiffness ratio of second storey to bottom storey γ . Calculating parameters of the structures are shown in Table 3.1.

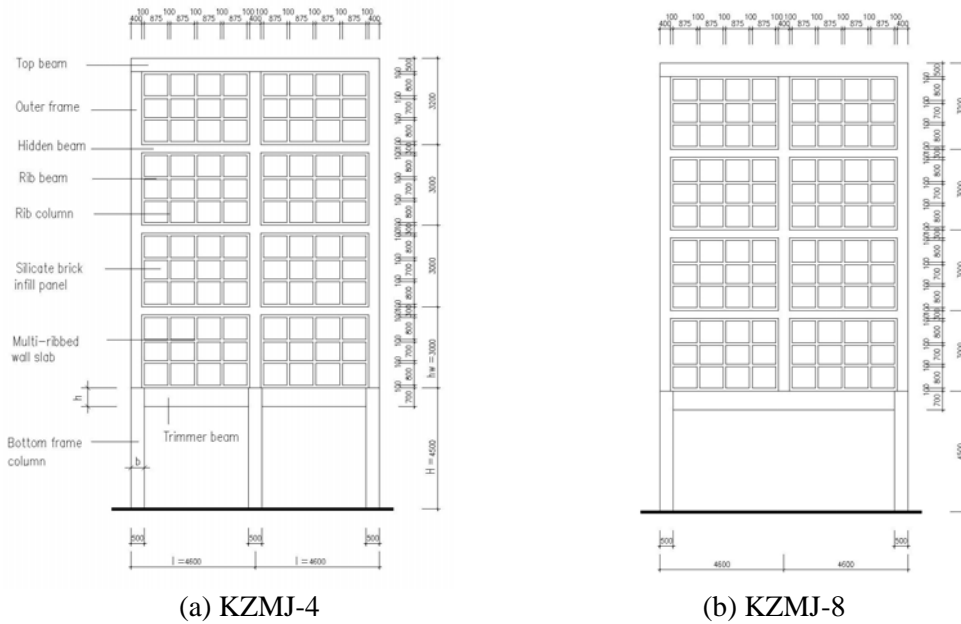


Figure 5 Elevation of calculating model

Table 3.1 Calculating parameters of the structures

Type	Dimension of post /mm	Width×highness of beam /mm	Span number	Span highness	h/l	b/l	b/H	h_w/l	γ
KZMJ-1	450×450	300×700	double	4.5	0.15	0.10	0.10	0.652	1.514
KZMJ-2	500×500	300×500	double	4.5	0.11	0.11	0.11	0.652	1.296
KZMJ-3	500×500	300×600	double	4.5	0.13	0.11	0.11	0.652	1.261
KZMJ-4	500×500	300×700	double	4.5	0.15	0.11	0.11	0.652	1.226
KZMJ-5	500×500	300×800	double	4.5	0.17	0.11	0.11	0.652	1.193
KZMJ-6	550×550	300×700	double	4.5	0.15	0.12	0.12	0.652	1.014
KZMJ-7	600×600	300×700	double	4.5	0.15	0.13	0.13	0.652	0.852
KZMJ-8	500×500	300×700	single	4.5	0.08	0.05	0.11	0.326	1.839
KZMJ-9	500×500	300×700	double	5.1	0.15	0.11	0.10	0.652	1.404
KZMJ-10	500×500	300×700	single	5.1	0.08	0.05	0.10	0.326	2.106
KZMJ-11	500×500	300×700	double	6.0	0.15	0.11	0.08	0.652	1.670
KZMJ-12	500×500	300×700	single	6.0	0.08	0.05	0.08	0.326	2.505
KZMJ-13	450×450	300×700	single	6.0	0.08	0.05	0.08	0.326	3.093
KZMJ-14	800×800	300×700	double	4.5	0.15	0.18	0.18	0.652	0.479

3.2 Result Analysis

3.2.1 Fundamental vibration characteristic

The nonlinear dynamic analysis of 14 model structures shows that the natural vibration periods (T) of frame-supported multi-ribbed slab structures are about 1.0~1.3s, belong to middling period. The first modal participation factor (Γ) is to get the most value (see Table 3.2), demonstrating the first mode make dominating effect. The first three modals show that along with increase of stiffness ratio(γ), or the more soft bottom storey of structures is, the more big displacement of bottom storey is, and there is a prominence in the bottom of modes, at the same time node location of modes transfer downwards, shown in Figure 6.

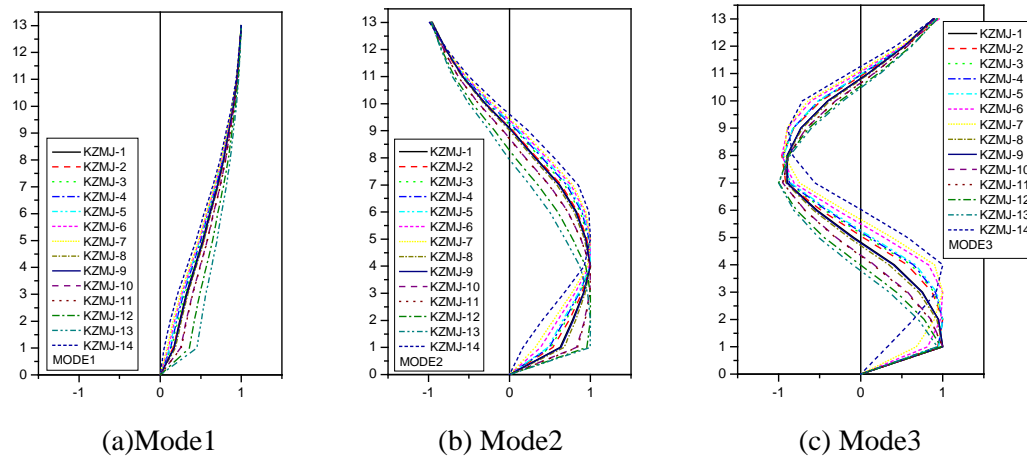


Figure 6 Modes of the structures

Table 3.2 Calculating results of first three modes

Type	mode	KZMJ -1	KZMJ -2	KZMJ -3	KZMJ -4	KZMJ -5	KZMJ -6	KZMJ -7	KZMJ -8	KZMJ -9	KZMJ -10	KZMJ -11	KZMJ -12	KZMJ -13	KZMJ -14
T/s	1 st	1.037	1.069	1.027	1.005	0.988	0.984	0.972	1.053	1.044	1.111	1.119	1.223	1.341	0.939
	2 nd	0.327	0.324	0.316	0.308	0.308	0.302	0.296	0.335	0.329	0.359	0.359	0.393	0.420	0.284
	3 rd	0.188	0.182	0.179	0.177	0.177	0.170	0.166	0.191	0.189	0.200	0.201	0.209	0.214	0.156
Γ	1 st	0.899	0.900	0.890	0.885	0.880	0.875	0.869	0.905	0.901	0.924	0.925	0.948	0.964	0.852
	2 nd	0.357	0.339	0.350	0.356	0.360	0.349	0.343	0.352	0.354	0.332	0.330	0.283	0.236	0.325
	3 rd	0.204	0.208	0.223	0.232	0.240	0.241	0.240	0.189	0.199	-0.146	-0.143	-0.097	-0.069	-0.216

3.2.2 Influence of earthquake ground motions

The maximum displacement and interstorey drift and acceleration responses of typical case KZMJ-4 under eight earthquakes with 0.4g are shown in Figure 7. The displacement and acceleration time-history responses of KZMJ-4 subjected to El-Centro, Taft, San Fernando and Kobe waves with 0.4g are shown in Figure 8~11. Computing time $t=30s$. Earthquake ground motions have big influence on seismic responses of the case. However, it reflects the same regularity as follows:

(1) The lateral displacement curves of the case present bending-shearing deformation characteristic where lower part of curves is close to bending and upper part of curves is close to shearing deformation.

(2) The maximum value of maximum interstorey drift transfer upwards which take place in the middle part of structures third storey but not in the second storey transition storey, showing that there is a combination act between the bottom frame trimmer beam and upper second storey multi-ribbed wall slab, or effect of wall-beam, so bring on the stiffness of transition storey increase and the deformation decrease. This combination effect of wall-beam is of advantage to develop seismic performance of frame-supported multi-ribbed slab structures.

(3) The acceleration and displacement time-history responses curves of KZMJ-4 show that there is a distinct dynamic interaction between stories of frame-supported multi-ribbed slab structures, and present obvious phase

difference. Because of mutual condition between stories, delivering and dissipating of energy, and growth and decline of vibration during the oscillating motion, so it brings on reducing of the earthquake responses of the structures. The maximum acceleration values change uniformity along highness of storey, average value of dynamic magnifying coefficient is lower than one.

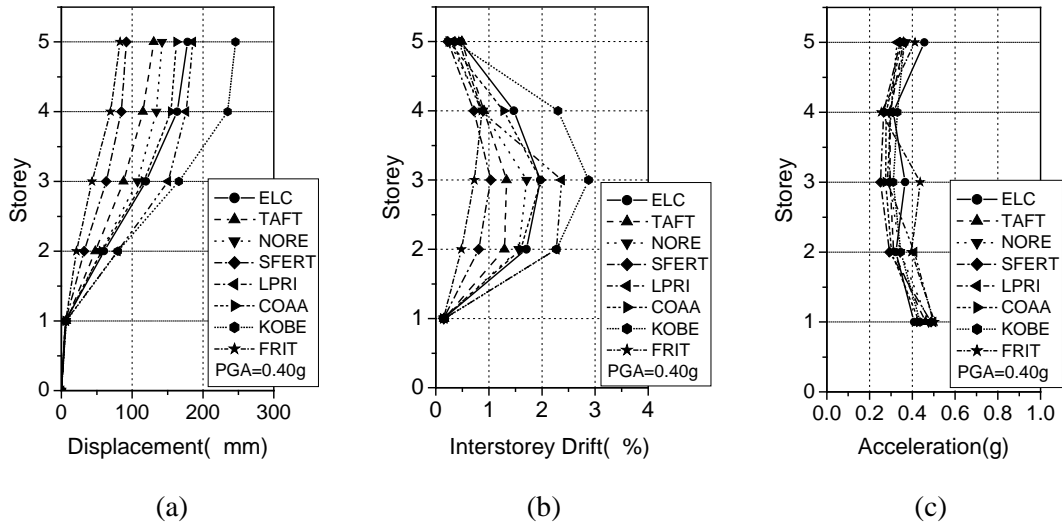
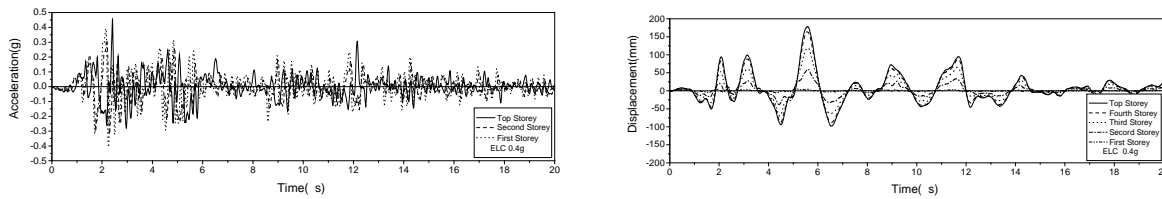


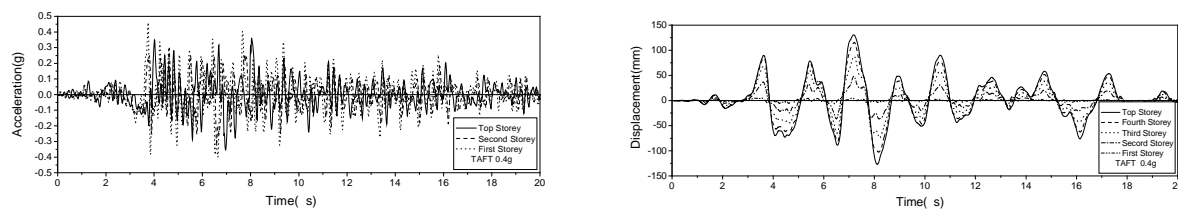
Figure 7 Maximum responses of KZMJ-4 under eight earthquakes with 0.4g



(a) Acceleration time-history curve

(b) Displacement time-history curve

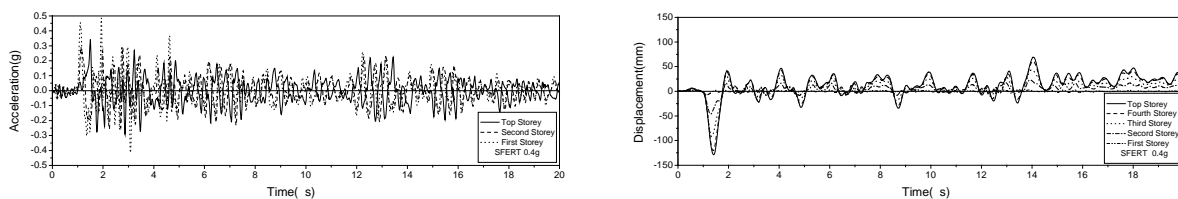
Figure 8 Time-history responses of KZMJ-4 subjected to El-Centro wave with 0.4g



(a) Acceleration time-history curve

(b) Displacement time-history curve

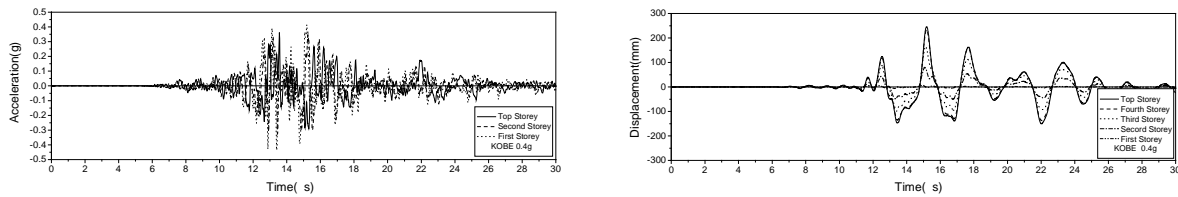
Figure 9 Time-history responses of KZMJ-4 subjected to Taft wave with 0.4g



(a) Acceleration time-history curve

(b) Displacement time-history curve

Figure 10 Time-history responses of KZMJ-4 subjected to San Fernando wave with 0.4g



(a) Acceleration time-history curve

(b) Displacement time-history curve

Figure 11 Time-history responses of KZMJ-4 subjected to Kobe wave with 0.4g

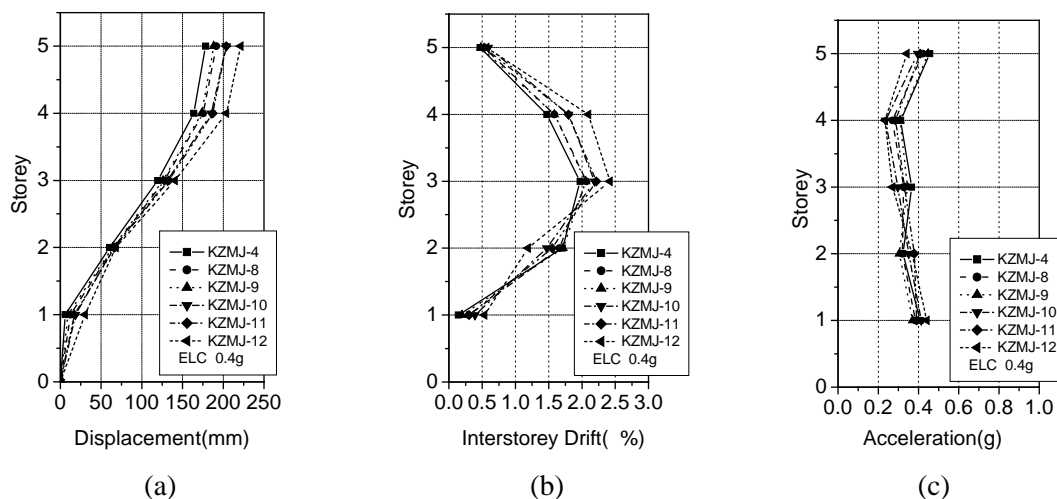
3. 2.3 Influence of analysis parameter

The change curves of maximum displacement and interstorey drift and acceleration responses of typical case KZMJ-4 subjected to El-Centro with 0.4g along with height to span ratio of trimmer beam h/l , width to span ratio of frame-supported columns b/l , width to highness ratio of frame-supported columns b/H , height to span ratio of second storey multi-ribbed wall slab h_w/l are given in Figure 12. It can be seen from Figure 12:

(1) When bottom frame of model structure changed from single span to double spans, or height to span ratio of trimmer beam h/l , width to span ratio of frame-supported columns b/l and height to span ratio of second storey multi-ribbed wall slab h_w/l are all reduced to about 1/2, for different width to highness ratio of frame-supported columns b/H , the lateral displacement curves of the case arises to change with increasing of lateral displacement of bottom frame and upper 3rd~5th storey of the structure, while there is a smaller deformation change of second storey multi-ribbed wall slab because of combination effect of wall-beam; the shearing deformation of the case has increased, especially in the bottom of structure. Not only single span but also double spans are still there a similar deformation characteristic above all when width to highness ratio of frame-supported columns b/H decreased.

(2) The distributing of maximum interstorey drift show that maximum interstorey drift of second storey multi-ribbed wall slab decrease while maximum interstorey drift of bottom frame and upper 3rd~5th storey of the structure increase along with reducing of h/l , b/l , b/H and h_w/l , which reflect the strengthening of combination effect of wall-beam.

(3) The distributing of acceleration responses show that maximum acceleration responses in the bottom frame storey increase while acceleration responses decrease in the upper 3rd~5th storey of the structure along with reducing of h/l , b/l , b/H and h_w/l , where second storey is provided with transition of acceleration.



(a)

(b)

(c)

Figure 12 Influence of analysis parameter

4. CONCLUSIONS

A rigid frame-oblique compression bar analytical macro-model based on an equivalent strut approach used for representing silicate brick infill panels was proposed in the nonlinear dynamic analysis of FSMRSS. The 8 natural earthquake ground motions were chosen respectively representing different frequency spectrum characteristic. The nonlinear dynamic time-history analysis of the numerical cases under earthquakes has been carried out. The results show that the lateral displacement curves of the cases present bending-shearing deformation features mainly being bending. The maximum interstorey drift take place in the upper multi-ribbed wall slab storey but not in the bottom frame-supported storey, which is of advantage to resist collapse of the structures. The acceleration and displacement time-history responses curves of KZMJ-4 show that there is a distinct dynamic interaction between stories of frame-supported multi-ribbed slab structures, while the maximum acceleration values change uniformity along highness and the average value of dynamic magnifying coefficient is lower than one. Sensitivity analysis of earthquake responses of the structures shows that influence of earthquake waves is the biggest, while height to span ratio of trimmer beam h/l , width to span ratio of frame-supported columns b/l , width to highness ratio of frame-supported columns b/H and height to span ratio of second storey multi-ribbed wall slab h_w/l have some influence.

REFERENCES

1. Scientific and Technical Report (2000). Study on Theory and Application of Multi-Ribbed Wall Slab Structure with Light-Weight Outer Frame, Xi'an University of Architecture & Technology, China.
2. Madan, A., Reinhorn, A.M., Mander, J.B. and Valles, R.E. (1997). Modeling of masonry infill panels for structural analysis. *Journal of Structural Engineering* 123:10, 1295-1302.
3. Reinhorn, A. M., Madan, A., Valles, R. E., Reichman, Y., and Mander, J.B. (1995). Modeling of masonry infill panels for structural analysis. Tech. Rep. NCEER-95-0018. Nat. Ctr. of Earthquake Engrg. Res., State University of New York, Buffalo, N.Y.
4. Saneinejad, A., and Hobbs, B. (1995). Inelastic design of infill frames. *J. Struct. Engrg., ASCE*. 121(4), 634-650.
5. Valles, R.E., Reinhorn, A.M., Kunnath, S. K., Li, C. and Madan, A. (1996). IDARC 2D version 4.0-a program for the inelastic damage analysis of buildings. Technical Report NCEER-96-0010, Nat. Ctr. for Earthquake Engrg. Res., State University of New York, Buffalo, N.Y.
6. Reinhorn, A.M., Valles, R.E. and Kunnath, S. K. (2006). IDARC 2D version 6.1-a program for the Inelastic Damage Analysis of Reinforced Concrete structures. State University of New York, Buffalo, N.Y.
7. Reinhorn, A.M., Valles, R.E. and Kunnath, S. K. (2006). IDARC 2D version 6.1- User's Guide. State University of New York, Buffalo, N.Y.
8. Sivaselvan, M.V. and Reinhorn, A.M. (1999). Hysteretic models for cyclic behavior of deteriorating inelastic structures. Technical Report MCEER-99-0018. State University of New York, Buffalo, N.Y.
9. GB50011-2001(2002). Code for seismic design of buildings, China Architecture & Building Press. Beijing, China.
10. DING Yong-gang. (2006). Research on load-bearing performance and design method of frame-supported multi-ribbed wall beam. PhD dissertation, School of Civil Engineering, Xi'an University of Architecture & Technology, Xi'an, China.
11. TIAN Jie. (2007). The nonlinear earthquake response analysis of frame-supported multi-ribbed slab structure and damage performance based seismic evaluation methods. PhD dissertation, School of Civil Engineering, Xi'an University of Architecture & Technology, Xi'an, China.